Available online at www.sciencedirect.com
SCIENCE DIRECT®
Bioelectrochemistry 60 (2003) 115–121
Bioelectrochemistry
www.elsevier.com/locate/bioelechem

Imaging of enzyme activity by scanning electrochemical microscope equipped with a feedback control for substrate–probe distance

Daisuke Oyamatsu, Yu Hirano, Norihiro Kanaya, Yoshiaki Mase, Matsuhiko Nishizawa, Tomokazu Matsue*

Department of Biomolecular Engineering, Graduate School of Engineering, Tohoku University, 07 Aramaki-Aoba, Sendai 980-8579, Japan

Received 20 December 2002; received in revised form 21 May 2003; accepted 27 May 2003

Abstract

The enzymatic activity of diaphorase (Dp) immobilized on a solid substrate was characterized using a scanning electrochemical microscope (SECM) with shear force feedback to control the substrate–probe distance. The shear force between the substrate and the probe was monitored with a tuning fork-type quartz crystal and used as the feedback control to set the microelectrode probe close to the substrate surface. The sensitivity and the contrast of the SECM image were improved in the constant distance mode (distance, 50 nm) with the shear force feedback compared to the image in the constant height mode without the feedback. By using this system, the SECM and topographic images of the immobilized diaphorase were simultaneously measured. The microelectrode tip used in this study was ground aslant like a syringe needle in order to obtain the shaper topographic images. This shape was also effective for avoiding the interference during the diffusion of the enzyme substrates.

Keywords: SECM; Diaphorase; Shear force; Feedback control

1. Introduction

In recent years, the development of analytical methods for biological materials such as enzymes and living cells has received much attention in advanced biotechnology. Among the various requirements for these analytical methods, acquiring the spatial distribution of the protein with a high sensitivity and selectivity is of particular importance for many applications such as enzyme-linked immnosorbent assays (ELISA) [1–3]. In the past, optical methods based on the fluorescence or chemiluminescence detection have commonly been used for this purpose. However, miniaturization of the optical instruments is difficult because of the complicated optical systems including lens, a photon detector, light source and dark chamber. In contrast, electrochemical probes have advantages of small size and simplicity. In particular, the scanning electrochemical microscope (SECM) has been found to be suitable for trace analyses required for biochips applications [4,5]. SECM is a kind of scanning probe microscope (SPM), which detects localized electrochemically active species to afford two- or three-dimensional images based on the distribution of these species [6]. However, a major drawback of the SECM is the difficulty in controlling the sample–probe distance, which decisively governs the sensitivity and the quality of the SECM image. SECM measurements have been conventionally done in the constant height mode, in which the microelectrode probe is scanned without a feedback loop to the probe tip. During imaging in the constant height mode, setting the probe tip close to a rough surface is difficult, resulting in low spatial resolution of the images.

Recently, the feedback distance control utilizing shear forces exerted between the probe and the sample has been applied to the scanning near-field optical microscope (SNOM). For the detection of shear force, many researchers have adopted the tuning fork-type quartz crystal resonators which have a relatively simple mechanism compared with an AFM-like system using an optical lever. For the SECM systems, a tuning fork quartz crystal has recently been used for feedback control of a microelectrode probe to afford the constant-distance imaging [7–10].

* Corresponding author. Tel./fax: +81-22-217-7209.
E-mail address: matsue@bioinfo.che.tohoku.ac.jp (T. Matsue).

1567-5394/03/$ - see front matter © 2003 Elsevier B.V. All rights reserved.
doi:10.1016/S1567-5394(03)00055-0

In this study, we use an SECM equipped with the feedback control system and imaged the enzymatic activities for immobilized diaphorase (Dp) in the constant distance mode. Diaphorase was detected by using ferrocenyl methanol (FMA) as the electron mediator. FMA was oxidized to FMA^+ at the microelectrode probe and diffused to the immobilized diaphorase, which catalyzed the oxidation of NADH to regenerate FMA. Since the reaction rate of this "redox cycling" is strongly influenced by the diffusion length of FMA and FMA^+, the distance between the microelectrode and the surface of the immobilized diaphorase is a decisive factor governing the sensitivity and quality of the SECM image. Electrochemical methods for the biochips based on the detection of enzymatic activities will be greatly improved by keeping the microelectrode very close to the surface in the constant-distance mode. In addition, since the vertical movement of the probe directly reflects the topography of the sample, the simultaneous measurement of the electrochemical and topographic information of the sample can be made by using the feedback distance control.

2. Experimental

2.1. Chemicals

Diaphorase (Dp) purified from *Bacillus stearothermophilus* (EC 1.6.99.-) was purchased from Unichika. This enzyme has a molar mass of about 30,000 and has one flavin mononucleotide (FMN) per molecule as an electroactive site [11]. Ferrocenylmethanol (FMA) was purchased from Aldrich Chemicals and recrystallized from hexane. All other chemicals including the β-nicotinamide-adenine dinucleotide, the reduced form (NADH, Orient Yeast), were used as received. All the solutions were prepared using purified water from a Milli-Q II system (Millipore).

2.2. SECM system equipped with the feedback distance control

The configuration of the SECM system with feedback control of sample–probe distance was basically the same as that reported by Büchler et al. [7]. The Pt microelectrode was attached to one of the legs of a tuning fork quartz crystal, which was commonly used as the time base of various types of watches. The resonance frequency of the unprocessed tuning fork was 32768 (2^{15}) Hz. The frequency dropped to about 28–30 kHz after attaching the microelectrode. The microelectrode and tuning fork quartz crystal were vibrated by a conventional piezoelectric buzzer for producing the sound. The buzzer was driven by an AC signal (50–100 mV p–p, sine wave) from the reference function generator equipped in a digital lock-in amplifier (NF, LI-5640). When the probe was positioned far from the substrate, the vibration from the buzzer induced a voltage signal in a tuning fork by a piezoelectric effect. The amplitude of the induced signal was several hundreds of microvolts, and its frequency was the same as the driving signal. The induced signal was detected by the digital lock-in amplifier. When the probe approaches the substrate and the distance becomes less than 100 nm, the shear force between the probe and the substrate decreases the magnitude of the vibration of the tuning fork. The drop in the induced signal was digitized and acquired by a 16-bit A/D converter (Interface, PCI-3178) equipped in the PCI bus of an IBM compatible PC. The feedback operation was conducted by the homemade software written by Microsoft Visual Basic 6.0. The feedback value was calculated by PI (proportional–integral) control equation shown as follows:

$$\Delta V_n = V_{\text{fork}} - V_{\text{setpoint}} \quad (1)$$

$$Z_n = Z_{n-1} + P(\Delta V_n - \Delta V_{n-1}) + I\Delta V_n \quad (2)$$

where V_{fork} is the input voltage from lock-in amplifier (0–5 V), V_{setpoint} is the target value of input voltage, ΔV_n is the present deviation of input voltage, ΔV_{n-1} is the previous deviation, Z_n is the vertical position of sample stage and Z_{n-1} is the previous vertical position. P and I are the coefficient of PI control and empirically set to 0.01 and 0.02, respectively. The calculating time of a step is faster than 100 μs (including the conversion time of A/D and D/A converter). Then, the vertical position of sample was controlled by a XYZ piezoelectric scanner (Physik Instrumente, P-517.3CL) so that the V_{fork} maintained a constant value (V_{setpoint}). The motion range of the scanner was 100× 100×20 μm. The stage was driven by a high-voltage power supply controlled by voltage signals (0–10 V) from a 16-bit D/A converter (Interface, PCI-3310).

The electrochemical measurements were conducted by controlling the electrode potential of the microelectrode versus an Ag|AgCl (sat. KCl) reference electrode and the current was detected by a highly gained current amplifier (Keithley, Model 427) and converted to digital data using the 16-bit D/A board.

2.3. Preparation of the probe

The probes for the SECM imaging with the feedback distance control (constant distance mode) were prepared using the following procedures. Since the tuning fork quartz crystal was sealed into an aluminum can to stabilize the resonance frequency, the can was first carefully removed from the tuning fork. The IC connector (1.78 mm pitch) was attached to the surface of piezoelectric buzzer, and the two terminals of tuning fork were firmly inserted into the IC connecter. The spattered patterns on the tuning fork were insulated with transparent enamel paint (Tamiya) to avoid any direct contact to the electrolyte solution.

The Pt wire (diameter=20 μm) was electrochemically etched by applying an AC voltage (10 V p–p, 300 Hz) in a

saturated $NaNO_3$ aqueous solution, and thermally sealed in a glass capillary. The resulting microelectrode was cut off at about 5 mm from the tip and glued to one of the legs of the tuning fork with cyanoacrylate cement. Finally, the tip of the microelectrode was ground aslant with a rotating diamond whetstone to obtain a shaper tip (acute angle at the tip was approximately 45°). The schematic illustration of the shape and size of the microelectrode tip was shown in Fig. 1.

2.4. Preparation of diaphorase-patterned substrate

The Au array electrodes were prepared on the slide glasses by a conventional photolithography method. The resulting substrates were immersed in a 1 mmol dm^{-3} octadecanethiol/ethanol solution for 8 h to form a self-assembled monolayer of the alkanethiol. The diaphorase was immobilized by physical adsorption on the SAM-modified substrate from the aqueous enzyme solution (0.15 mg/ml diaphorase).

2.5. SECM imaging of diaphorase activity

Fig. 2 shows a schematic diagram of the redox reaction between the microelectrode probe and the diaphorase-immobilized surface. Diaphorase catalyzes the electron transfer from NADH to a suitable acceptor molecule. In the present system, FMA, an electron mediator, is oxidized to FMA^+ at the microelectrode probe (0.5 V vs. Ag|AgCl) and FMA^+ diffused to the immobilized diaphorase. The diaphorase

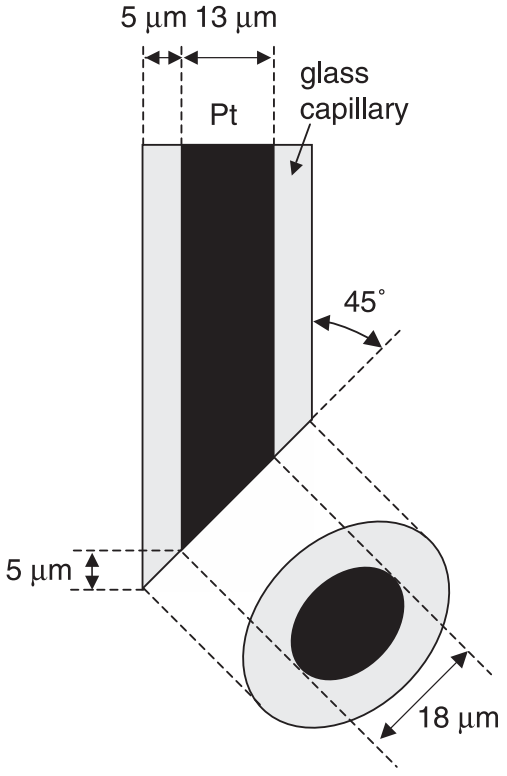

Fig. 1. The shape and size of the microelectrode used in this study.

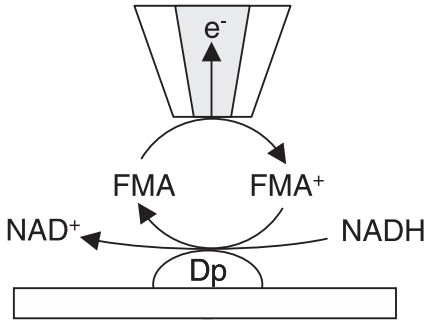

Fig. 2. Schematic diagram of the diaphorase-catalyzed reaction.

catalyzes the oxidation of NADH to regenerate FMA, which diffuses to the probe and is oxidized again at the probe. This "redox cycling" between the electrode tip and the substrate surface increases the oxidation current of FMA.

3. Results and discussion

3.1. Characterization of the SECM probes

Fig. 3a shows the typical dependency of the amplitude of the induced signal on the vibration frequency for the prepared SECM probe. Since the absolute amplitude of the induced signals was different from each probe, the amplitude was expressed by an arbitrary unit. As shown in this figure, the maximum amplitude was observed at the frequency of 30.84 kHz, which would correspond to the mechanical resonance of the tuning fork. Although this frequency showed little scattering for each tuning fork probe, it was slightly lower than the resonance frequency of the unprocessed tuning fork quartz crystal (=32.768 kHz). The decrease in frequency was due to the addition of the extra mass of the microelectrode to the leg of the tuning fork. During the control of the sample–probe distance, the vibration frequency was adjusted to the resonance frequency of the individual probes. The quality of the tuning fork can be roughly evaluated from the shape of the peak resonance frequency. The probes showing sharper peaks have a tendency to have a better sensitivity in topography imaging of the sample surface. In this measurement, the amplitude of the driving signal applied to the piezoelectric buzzer for the vibration of the probe was 50–100 mV. Since the amplitude of the induced signal depends on the magnitude of the vibration, the detection of the induced signal becomes easier at high driving voltages. However, excess vibration of the microelectrode may reduce the accuracy of the electrochemical responses since the vibration interferes with the diffusion of the electrochemically active species to the microelectrode.

Fig. 3b shows the change in the amplitude of the induced signal in the tuning fork obtained during an approach of the microelectrode to the substrate surface. As reported by Büchler et al. [7], the amplitude of the induced signals decreases when the probe approaches the surface within

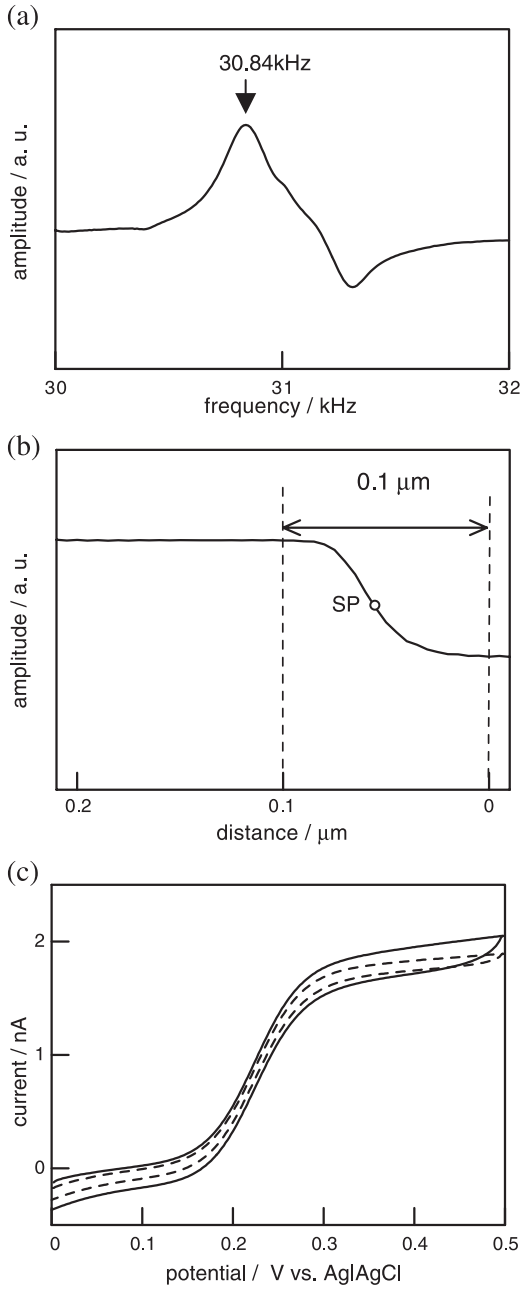

Fig. 3. (a) Relationship between the vibration frequency of the tuning fork quartz crystal and the amplitude of the induced signal. (b) Relationship between the sample–probe distance and the amplitude of the induced signal. (c) Cyclic voltammograms of the static (dashed line) and vibrating (solid line) microelectrodes obtained in an aqueous solution containing 1 mmol dm^{-3} FMA, 0.1 mol dm^{-3} KCl and 0.1 mol dm^{-3} Na_2HPO_4 at the scan rate of 20 mV s^{-1}.

100 nm. Once the probe touched the surface, the amplitude was almost unchanged thereafter. The amplitude of the induced signal was used for the feedback control of the *z*-position of XYZ stage in order to maintain a constant probe–surface distance. In this study, the amplitude was set to the point SP shown in Fig. 3b, the middle amplitude between the amplitudes at 100 and 0 nm distances. Thus, the position of the probe was maintained at about 50 nm above the substrate surface. The vibration of the microelectrode by the piezoelectric buzzer induces slight increase in the current responses by about 9% (Fig. 3c) probably due to light disturbance of the diffusion region at the electrode. This slight increase has no serious problem in imaging of the enzyme activities.

3.2. SECM imaging of diaphorase-immobilized substrate with feedback distance control

Fig. 4a shows the SECM image of diaphorase immobilized on the Au array electrode obtained in the NADH-free electrolyte solution (1 mmol dm^{-3} FMA, 0.1 mol dm^{-3} KCl and 0.1 mol dm^{-3} Na_2HPO_4). The sample–probe distance was stabilized at 50 nm with the feedback control. The slight increase of oxidation current was observed above the Au array electrode. It would be due to the redox cycling reaction of FMA/FMA^+ between the microelectrode and the Au array through the defects of the octadecanethiol SAM.

Fig. 4b shows the SECM image of diaphorase immobilized on the Au array electrode obtained in the constant height mode (without the feedback control of the probe–substrate distance) after addition of 5 mmol dm^{-3} NADH. The initial distance was set to 3 μm, although the actual distance was influenced by the tilt or undulation of the substrate. The addition of NADH to the solution resulted in a significant increase in the oxidation current due to the redox cycling induced by the enzymatic reaction of diaphorase in the diaphorase-immobilized areas, showing a striped pattern in the SECM image. In the constant height mode, the border lines of the stripes were not very clear due to the diffusional influence of FMA from the immobilized enzymes to the microelectrode. Such an undesired diffusional influence becomes significant as the probe–substrate distance increases.

The SECM image (Fig. 4c) obtained in the constant distance mode (probe–substrate distance: 50 nm) is apparently clear compared with the image shown in Fig. 4b. The oxidation current above the diaphorase-immobilized area is greater than that obtained without feedback control. In addition, the contrast of the SECM image was significantly improved. Fig. 4d shows the current response along the line A–B in Fig. 4a–c. With the feedback control, the oxidation current at the diaphorase-immobilized line was about two times larger than that without feedback control. The response of the oxidation current is caused by the redox cycling, and therefore, shortening the diffusion length between the microelectrode and the immobilized diaphorase increases the oxidation current. The oxidation current above the glass part is, however, significantly lower than that without the feedback control. Since the electrode is very close to the surface in the feedback mode, the diffusion of FMA to the microelectrode is quite hindered, lowering the oxidation current. Because of the efficient redox cycling at the enzyme-immobilized line and the blockage effect of the diffusion at the glass area, the contrast of the SECM image

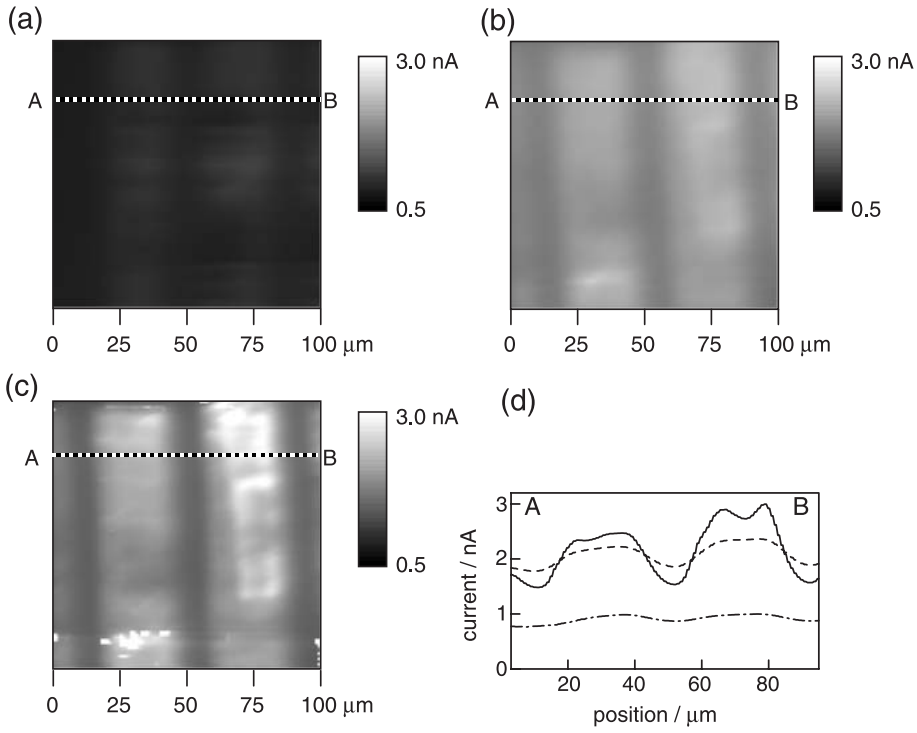

Fig. 4. (a) SECM images of diaphorase immobilized on the Au array electrodes obtained in the NADH-free solution. The sample–probe distance was stabilized at 50 nm with the feedback control. (b) SECM images of same sample obtained after addition of 5 mmol dm^{-3} NADH without the feedback control. The initial sample–probe distance was about 3 μm. (c) SECM images of same sample obtained after addition of 5 mmol dm^{-3} NADH. The sample–probe distance was stabilized at 50 nm with feedback control. (d) Cross-sectional view of oxidation current along the line A–B shown in (a) (dotted and dashed line), (b) (dashed line) and (c) (solid line). Scan rate of microelectrode: 10 μm s^{-1}. Electrode potential: +0.5 V vs. Ag|AgCl. Measurement solution: 1 mmol dm^{-3} FMA, 5 mmol dm^{-3} NADH, 0.1 mol dm^{-3} KCl and 0.1 mol dm^{-3} Na_2HPO_4.

was improved by using the feedback control system to place the probe very close to the substrate.

3.3. Current-distance curves (approach curves)

Fig. 5 shows the approach curves which are the change in the oxidation current during the approach of the probe to the diaphorase-immobilized and the glass areas. As expected from the results in Fig. 4c, the oxidation current monotonically increased as the probe approached the Dp-modified substrate. The previous study [12] reported that in the approach curve, the oxidation current first increased, but rapidly decreased when the probe–substrate distance was less than one-tenth of the tip diameter. This rapid decrease was attributed to interference of the microelectrode itself to the diffusion of NADH from the bulk solution to the immobilized enzyme. This difference in the current profile between the present study and the previous result is caused by the difference in the tip shape of the probe. During normal SECM measurements, the tip surface is aligned parallel to the substrate. When such a microelectrode approaches the flat surface, the clearance between the microelectrode and the substrate becomes too narrow to allow the diffusion of the substrates toward the immobilized

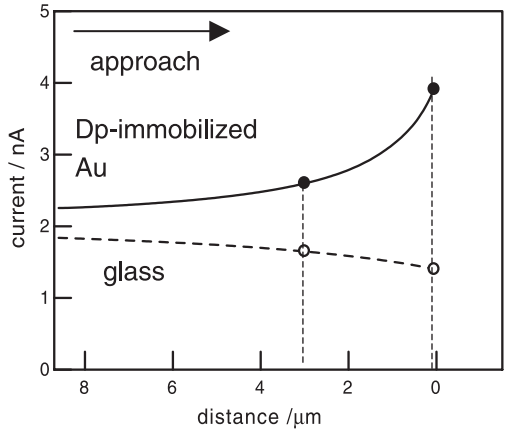

Fig. 5. Relationship between the sample–probe distance and the oxidation current on the diaphorase-immobilized Au electrodes (solid line) and the glass substrate (dashed line). Electrode potential: +0.5 V vs. Ag|AgCl. Measurement solution: 1 mmol dm^{-3} FMA, 5 mmol dm^{-3} NADH, 0.1 mol dm^{-3} KCl and 0.1 mol dm^{-3} Na_2HPO_4.

Table 1
Current responses measured above the immobilized diaphorase and the glass substrate at the sample–probe distance of 3 and 0.05 μm, respectively

Distance (μm)	Oxidation current above the immobilized diaphorase (nA)	Oxidation current above the glass (nA)	Current ratio
3.0	2.60	1.65	1.58
0.050	3.91	1.40	2.79

The current ratios calculated from these values are also shown in this table.

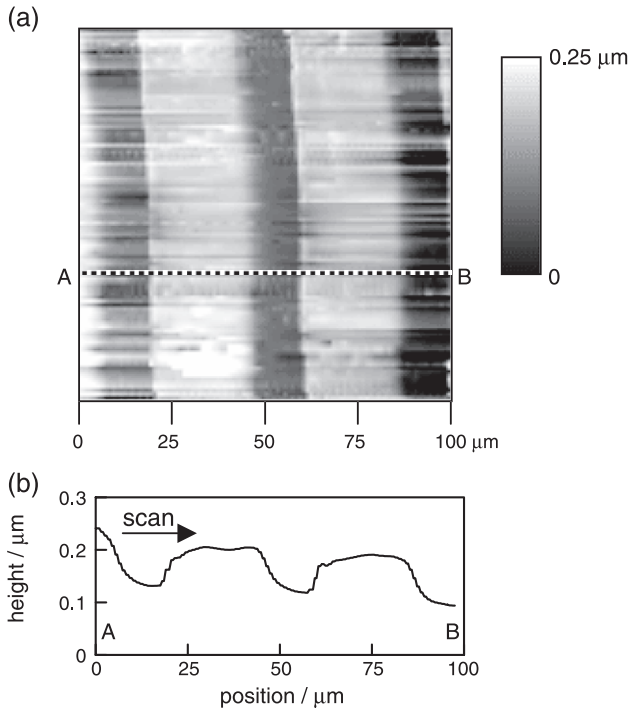

Fig. 6. (a) Topographic image of diaphorase-immobilized Au array electrodes simultaneously obtained with the SECM image shown in Fig. 4c. (b) Cross-sectional view of the topography along with the line A–B shown in (a).

enzyme. In the present study, the tip of the probe was diagonally ground with an acute angle (45°) to the central axis to make a sharper tip. This tip shape ensures enough clearance for the diffusion of the substrates even if the probe is less than 50 nm. Table 1 shows the oxidation current at the diaphorase-immobilized and the glass areas. When the probe was positioned 3 μm above the surface, the ratio of the oxidation current above the immobilized diaphorase to that above the glass substrate was 1.58. The current ratio increased to 2.79 at the 50-nm distance. This increase in the ratio reinforces the enhancement of the contrast in the SECM images with feedback control of the sample–probe distance. The quantitative investigation of the diffusion at the slanting tip using simulation will be reported elsewhere.

In the SECM imaging with the feedback control, the height of the sample stage was continuously controlled to maintain a constant sample–probe distance. Therefore, the three-dimensional topography of the sample surfaces can be simultaneously obtained with the SECM image by recording and plotting the vertical movement of the sample stage. Fig. 6a shows the topographic image simultaneously obtained with the SECM image shown in Fig. 4c. The band structure of the Au array electrode was clearly represented. The thickness of the Au layer was obtained from a cross-sectional view of the image along the line A–B (Fig. 6b) and found to be about 100 nm, which was in good agreement with that measured by a meter thickness just after the preparation of the Au array electrode. The fuzziness of the Au array edges is due to the delay in the vertical movement at the stage or the insufficient sharpness of the probe tip. A slower scan speed and higher feedback sensitivity would minimize such a delay in the movement to afford clear images, although the slower scan takes longer measurement times and the excess feedback sensitivity may cause an undesirable oscillation of the system. For a fundamental solution, the microelectrode probe should be fine and stiff in order to transmit effectively the shear force from the microelectrode tip to the tuning fork quartz crystal.

4. Conclusions

Diaphorase immobilized on the Au array electrode was imaged with an SECM system equipped with the feedback control of the sample–probe distance by monitoring the shear force exerted between the sample and the probe. The feedback control system allows the microelectrode probe to move closer without hitting the sample surface. The SECM measurement of the immobilized enzyme provided information on the enzymatic activity in the local area of the sample. The current response increased as the microelectrode probe approached the diaphorase-immobilized area due to the catalyzed redox cycling (positive feedback). In contrast, the current response decreased as the probe approached the glass substrate due to the diffusion-blocking effect (negative feedback). Therefore, the sensitivity and contrast of the SECM image was significantly enhanced when the probe was positioned at a 50-nm distance with feedback control. In addition, the topographic image of the diaphorase-immobilized substrate was obtained by monitoring the vertical movement of the sample stage. The probe tip used in this study was ground to an acute angle like the needle of a syringe. The sharpened probe provided a better topographic image and minimized the undesired interference of the diffusion of the substrates. The enhanced sensitivity and contrast in the SECM images will be particularly useful for characterization of biomaterials such as enzymes and living cells.

Acknowledgements

This work was supported by a Grant-in-Aid for Priority Area 417 (No. 14050010) and a Grant-in-Aid for the Creation of Innovations through Business–Academic–Public Sector Cooperation (No. 13504) from the Ministry of Education, Culture, Sports, Science and Technology, Japan.

References

[1] G. Macbeath, S.L. Schreiber, Printing proteins as microarrays for high-throughput function determination, Science 289 (2000) 1760–1763.

[2] B. Schweitzer, S.F. Kingsmore, Measuring proteins on microarrays, Current Opinion in Biotechnology 13 (2002) 14–19.
[3] T.O. Joos, D. Stoll, M.F. Templin, Miniaturized multiplexed immunoassays, Current Opinion in Chemical Biology 6 (2001) 76–80.
[4] H. Shiku, T. Matsue, I. Uchida, Detection of microspotted carcinoembryonic antigen on a glass substrate by scanning electrochemical microscopy, Analytical Chemistry 68 (1996) 1276–1278.
[5] H. Shiku, Y. Hara, T. Matsue, I. Uchida, T. Yamauchi, Dual immunoassay of human chorionic gonadotropin and human placental lactogen at a microfabricated substrate by scanning electrochemical microscopy, Journal of Electroanalytical Chemistry 438 (1997) 187–190.
[6] A.J. Bard, F.R.F. Fan, J. Kwak, O. Lev, Scanning electrochemical microscopy. Introduction and principles, Analytical Chemistry 61 (1989) 138–144.
[7] M. Büchler, S.C. Kelley, W.H. Smyrl, Scanning electrochemical microscopy with shear force feedback, Electrochemical and Solid-State Letters 3 (2000) 35–38.
[8] A. Hengstenberg, A. Blöchel, I.D. Dietzel, W. Schuhmann, Spatially resolved detection of neurotransmitter secretion from individual cells by means of scanning electrochemical microscopy, Angewandte Chemie, International Edition 40 (2001) 905–908.
[9] Y. Zu, Z. Ding, J. Zhou, Y. Lee, A.J. Bard, Scanning optical microscopy with an electrogenerated chemiluminescent light source at a nanometer tip, Analytical Chemistry 73 (2001) 2153–2156.
[10] Y. Lee, Z. Ding, A.J. Bard, Combined scanning electrochemical/optical microscopy with shear force and current feedback, Analytical Chemistry 74 (2002) 3634–3643.
[11] T. Matsue, H. Yamada, H. Chang, I. Uchida, Electrooxidation of NADH with $Co(phen)_3^{3+}$ by NADH dehydrogenase purified from *Bacillus stearothermophilus*, Bioelectrochemistry and Bioenergetics 25 (1990) 347–354.
[12] H. Yamada, H. Shiku, T. Matsue, I. Uchida, Determination of active diaphorase immobilized at electrode surfaces, Bioelectrochemistry and Bioenergetics 29 (1993) 337–346.